Author Manuscript

Author Manuscript

Author Manuscript

Author Manuscript

HHS Public Access

Author manuscript

Phys Status Solidi B Basic Solid State Phys. Author manuscript; available in PMC 2017 February 01.

Published in final edited form as:

Phys Status Solidi B Basic Solid State Phys. 2016 August ; 253(8): 1494–1497. doi:10.1002/pssb.201600135.

II–VI Quantum Cascade emitters in the 6–8μm range

Thor A. Garcia[1,4], **Joel De Jesus**[2,4], **Arvind P. Ravikumar**[3], **Claire F. Gmachl**[3], and **Maria C. Tamargo**[1,4]

[1]Department of Chemistry, The City College of New York, 85 St. Nicolas Terrace, New York, New York 10031 USA

[2]Department of Physics, The City College of New York, 85 St. Nicolas Terrace, New York, New York 10031 USA

[3]Department of Electrical Engineering, Princeton University, Princeton, New Jersey 08544 USA

[4]The Graduate Center, City University of New York, New York, New York 10016, USA

Abstract

We present the growth and characterization of ZnCdSe/ZnCdMgSe quantum cascade (QC) heterostructures grown by molecular beam epitaxy (MBE) and designed to operate at 6-8μm. These structures utilize the better-understood ZnCdMgSe with InP lattice matched compositions yielding a bandgap of 2.80 eV as compared to previous work which used ZnCdMgSe compositions with bandgaps at 3.00 eV. Grown structures posses good structural and optical properties evidenced in X-ray diffraction and photoluminescence studies. Fabricated mesa devices show temperature dependent I-V measurements with differential resistance of 3.6 Ω, and a turn on voltage of 11V consistent with design specifications. Electroluminescence was observed in these devices up to room temperature with emission centered at 7.1 μm and line widths of ~16%(ΔE/E) at 80K. The results show that these are well-behaved electroluminescent structures. Addition of waveguide layers and further improvements in well barrier interfaces are being pursued in efforts to demonstrate lasing.

Keywords

Quantum Cascade Lasers; II-VI; Mid-IR; Semiconductor Lasers

1 Introduction

Since they were first demonstrated in 1994[1], quantum cascade (QC) lasers have had great success using the AlInAs/InGaAs/InP material system. Although that material system offers a great deal of flexibility through band engineering there are some limits imposed by the material system, such as the conduction band offset (CBO), which limits the emission wavelength to values above 4μm. In order to overcome these limits and to achieve a broader range of performance options, novel material systems are being investigated. These new systems include Antimony based[2], GaN based, Si based[3] and II-VI based

Correspondence to: Maria C. Tamargo.

Author Manuscript Author Manuscript Author Manuscript Author Manuscript

semiconductors, each at various levels of development. Currently the ZnCdSe/ZnCdMgSe material system remains one of the most promising. ZnCdSe/ZnCdMgSe has a direct bandgap, no intervalley scattering and a CBO as high as 1.12 eV[4] making it a good candidate for devices operating in a broad range of infrared wavelengths[5,6,7] including wavelengths as low as 1.55 μm. We have previously reported electroluminescence in this material system in the 4 to 5 μm range [6,7]. However, lasing from structures made from this system has not yet been observed, likely due to non-optimized materials properties. In order to understand and possibly overcome the absence of lasing we propose to design and grow devices to operate in the 6-8 μm range. This wavelength range relaxes the design requirements and it allows for the use of a 2.80 eV bandgap ZnCdMgSe barrier layer, which has a lower Mg content than the previously used composition with a 3.00 eV bandgap. This new composition has well-studied material parameters and is easier to grow in high quality[8]. The simplified design specification, presented in figure 1, which also includes shorter injector regions and thus fewer layers, generally allows for the study of problems related to performance present in the more technologically challenging short wavelength devices[7]. This path mirrors the development of QC devices in III-V materials in the early stages of development. In this work we explore the molecular beam epitaxy (MBE) growth and characterization of a structure designed for emission centered at 6.5μm. This structure incorporates a three-well, bound-to-bound active region and short injector design [9] as a first step in the demonstration of long wavelength II-VI based QC laser devices.

2 Experiment

2.1 MBE Growth

The samples were grown by molecular beam epitaxy (MBE) on (001) S doped InP substrates having carrier concentrations of $1 \times 10^{17} cm^{-3}$. Growth was performed utilizing a dual chamber Riber 2300P system equipped with in-situ reflection high-energy electron diffraction (RHEED). The samples were grown by first deoxidizing the surface of epi-ready InP (001) in a chamber dedicated to the growth of III-V materials. Following deoxidation, an $In_{0.53}Ga_{0.47}As$ layer doped with Si ($n \sim 1 \times 10^{18}$ cm^3) was grown with a thickness of ~250 nm at a nominal temperature of 500°C. The as grown $In_{0.53}Ga_{0.47}As$ layer was prepared with an As rich β(2×4) surface reconstruction. Samples where cooled to room temperature and then transferred via ultra-high vacuum transfer modules to a chamber dedicated to the growth of II-VI materials where the substrate temperature was raised to 170°C. There, the surface was exposed to a Zn flux for 30 seconds, followed by the growth of a $Zn_{0.53}Cd_{0.47}Se$ 10 nm thick buffer layer at 170°C. The substrate temperature was then raised to a nominal temperature of 280°C and the rest of the structure was grown with a Se stabilized (2×1) surface reconstruction. All layers where engineered to be less than 0.2% mismatched to the InP substrate to prevent the formation of dislocations and rock salt phase separation of Mg containing alloys[10].

2.2 Device Design

The design layer sequence in angstroms of one period of the active-injector region, beginning with the thickest well and repeated 40 times, is as follows: **42**/10/**34**/10/**26**/10/**21**/12/**15**/12/**14**/12 with the ZnCdSe well layers designated in boldface

Author Manuscript Author Manuscript Author Manuscript Author Manuscript

and Cl-doped ($n\sim3\times10^{17}$ cm^{-3}) layers underlined. The conduction band profile for two repeats of an active-injector region is shown in figure 1. For the core region, $Zn_{0.33}Cd_{0.3}Mg_{0.37}Se$ layers with Eg = 2.83eV were employed. At the interface between barriers and wells, 20s growth interruptions with a Se overpressure were incorporated into the growth sequence to improve the interface quality [7]. The complete sample design beginning at the bottom of the structure is as follows, 300 nm $In_{0.53}Ga_{0.47}As$ buffer, 10nm $Zn_{0.5}Cd_{0.5}Se$ buffer, a 400 nm $Zn_{0.5}Cd_{0.5}Se$:Cl ($n\sim3\times10^{17}$), the active core described above, 200 nm $Zn_{0.5}Cd_{0.5}Se$:Cl ($n\sim3\times10^{17}$) layer and a 200 nm $Zn_{0.5}Cd_{0.5}Se$:Cl highly doped ($n\sim1\times10^{18}$) contact layer.

2.3 Characterization

High-resolution x-ray diffraction (HR-XRD) measurements were made with a Bruker D8 Discover with DAVINCI design. Photoluminescence (PL) measurements were made with an Omnichrome He-Cd laser at a wavelength of 325 nm using a HR4000 Ocean Optics spectrometer. To observe the PL emission from the active core, samples were etched with a 1% bromine-methanol solution to remove the upper layers prior to the measurement. Electroluminescence measurements were preformed utilizing a Thermo-fisher 8700 Fourier transform infrared (FT-IR) spectrometer in step scan mode with a lock-in amplifier. All presented electroluminescence spectra are taken with a ZnSe polarizer set to transverse magnetic(TM), and then repeated at 90°, transverse electric(TE), to verify intersubband(ISB) origin. A liquid nitrogen cooled mercury cadmium telluride detector was used to measure the emitted light. Devices where fabricated in to 250μm half circular cleaved mesas by optical lithography and wet etching.

3 Results/Discussion

3.1 X-ray Diffraction

High resolution x-diffraction (HR-XRD) measurements of the sample are presented in figure 2a. This measurement shows strong and sharp satellite peaks consistent with the high quality of the structure grown. In these measurements we observed full with at half maximum (FWHM) of 95 arc seconds for the zero order superlattice as calculated from a polynomial fit to superlattice fringes. The identity of the $In_{0.53}Ga_{0.47}As$ peak was determined utilizing a calibration sample grown the same day with the same growth conditions (not shown). Once the zeroth order SL peak was identified, the remaining peak was assigned to the $Zn_{0.5}Cd_{0.5}Se$ layers. This assignment was in agreement with the energy dependence of PL measurements. HR-XRD (004) measurements show the lattice mismatch of -0.15% for $Zn_{0.5}Cd_{0.5}Se$, 0.02% for $In_{0.53}Ga_{0.47}As$, and 0.09% for the active core. Close lattice matching to the InP substrate is necessary to prevent misfit dislocations. X-ray reflectance (XRR) studies on the sample (figure 2c) gives a period of 24.7 nm. The discrepancy between the design and measured period is due to a somewhat faster growth rate than calibrated and a shutter error in the growth of the 42Å well, making it ~54Å thick. This error also led to a shift in the operating bias and wavelength of the device. XRR measurements show good interface quality for II-VI materials in the active core and throughout the structure.

Author Manuscript Author Manuscript Author Manuscript Author Manuscript

3.2 Photoluminescence

Photoluminescence measurements (figure 3) show the optical characteristics of the structure as one traverses along the growth direction by the use of etching to reveal the lower lying layers. Strong sharp PL emission is observed in each region of the sample originating from the different layers in the structure, consistent with high quality material. We only observe a weak deep level emission in the sample etched for the longest time, suggesting that it originates from defects near the heterovalent interface. The FWHM of the bottom $Zn_{0.5}Cd_{0.5}Se$ layer is 24 meV and 31 meV for the top $Zn_{0.5}Cd_{0.5}Se$ layer. Both top and bottom $Zn_{0.5}Cd_{0.5}Se$ layers have a bandgap near 2.16 eV at 77K. The active core has a bandgap near 2.24 eV at 77K and a FWHM of 24 meV. A FWHM of 24 meV for the active core shows the material to be of high quality, similar to that of single quantum wells in high quality materials, and shows there is uniformity in thickness of the quantum wells across the structure[11]. The linewidths for the top and bottom $Zn_{0.5}Cd_{0.5}Se$ bulk layers are consistent with our best II-VI material quality measured at 77K[7].

3.2 Device Performance

Pulsed I-V measurements of fabricated mesa devices done at 5 kHz (100 ns pulse width) are presented in figure 4a. We observe low differential resistance (3.2 Ω at 300K) indicative of very good electrical properties, comparable with III-V devices of similar design. Measured turn on voltage of 11 V is consistent with the design.

Electroluminescence(TM) measurements performed at 80 kHz (200ns pulse width) as a function of current (figure 4b) and temperature (figure 4c) show a Gaussian lineshape with a peak centered at ~7.1μm up to 160K. Linewidths of ~16%(ΔE/E) at 80K are observed, which are somewhat wider than those typically seen on III-V materials. The peak at 7.1μm goes to zero when the polarizer is rotated 90° verifying its ISB origin. At about 180K a second peak is observed that is not polarization dependent suggesting it is of thermal origin. This peak dominates the spectra at higher currents, so spectra taken at 1A are presented above 180K. A better understanding of the origin of this peak is being pursued. Emission from the 7.1μm peak persists up to 280K. The presence of ISB electroluminescence up to room temperature will enable us to investigate further the optimization of the QC laser structure with these materials.

4 Conclusions

We have shown the detailed materials properties and electroluminescence characteristics of the first reported II-VI long-wave (7.1μm) QC emitter. The QC design was optimized and made robust by using a lower bandgap ZnCdMgSe quaternary barrier layer as well as short-injector regions. MBE growth of a high quality structure was carried out and observed to exhibit excellent II-VI crystal quality both optically and structurally. Fabricated devices showed best-reported I-V characteristics for II-VI materials QC structures, with the expected turn on voltage and low differential resistance. Electroluminescence at 7.1 μm was observed up to 280 K. The results suggest that these structures are good candidates to pursue lasing from these materials. Future work involves design and growth of full devices, with

Author Manuscript Author Manuscript Author Manuscript Author Manuscript

waveguide ZnCdMgSe/ZnCdSe layers, which are expected to lead to the demonstration of lasing from these materials.

Acknowledgments

This material is based upon work supported by the National Science Foundation under Grant No. EEC-0540832 (MIRTHE) and Grant No. HRD-0833180 (CENSES). T. A. G. also acknowledges support from the RISE program at CCNY.

References

1. Faist J, Capasso F, Sivco DL, Sirtori C, Hutchinson AL, Cho AY. Science. 1994; 264:553. [PubMed: 17732739]
2. Teissier R, Barate D, Vicet A, Alibert C, Baranov AN, Marcadet X, Renard C, Garcia M, Sirtori C, Revin D, Cockburn J. Appl Phys Lett. 2004; 85:167.
3. Bates R, Lynch SA, Paul DJ, Ikonic Z, Kelsall RW, Harrison P, Liew SL, Norris DJ, Cullis AG, Tribe WR, Arnone DD. Appl Phys Lett. 2003; 83:4092.
4. Sohel M, Zhou X, Lu H, Perez-Paz MN, Tamargo M, Muñoz M, Vac J. Sci Tech B. 2005; 23:1209.
5. Franz KJ, Charles WO, Shen A, Hoffman AJ, Tamargo MC, Gmachl C. Appl Phys Lett. 2008; 92:121105.
6. Yao Y, Alfaro-Martinez A, Franz KJ, Charles WO, Shen A, Tamargo MC, Gmachl CF. Appl Phys Lett. 2011; 99:041113.
7. Garcia TA, de Jesus J, Ravikumar AP, Hong S, Shen A, Gmachl CF, Tamargo M, Vac J. Sci Technol B. 2013; 31:03C133.
8. Zeng L, Yang B, Tamargo M, Snoeks E, Zhao L. Appl Phys Lett. 1998; 72:1317.
9. Franz KJ, Liu PQ, Raftery JJ, Escarra MD, Hoffman AJ, Howard SS, Yao Y, Dikmelik Y, Wang X, Fan JY, Khurgin JB. Elec Lett. 2010; 46:591.
10. Moug RT, Sultana H, Yao Y, Alfaro-Martinez A, Peng L, Garcia T, Shen A, Gmachl C, Tamargo MC. J Electron Mater. 2012; 41:944.
11. Cavus A, Zeng L, Tamargo MC, Bambha N, Semendy F, Gray A. Appl Phys Lett. 1996; 68:3446.

Author Manuscript Author Manuscript Author Manuscript Author Manuscript

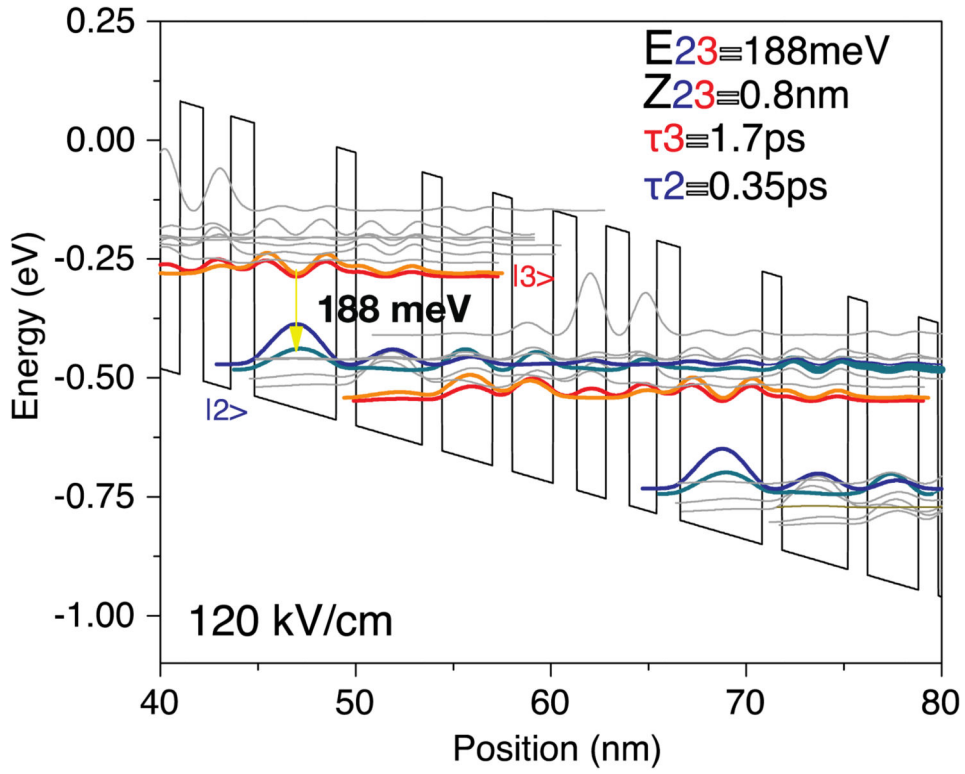

Figure 1.
Band diagram of active core design used in device.

Author Manuscript Author Manuscript Author Manuscript Author Manuscript

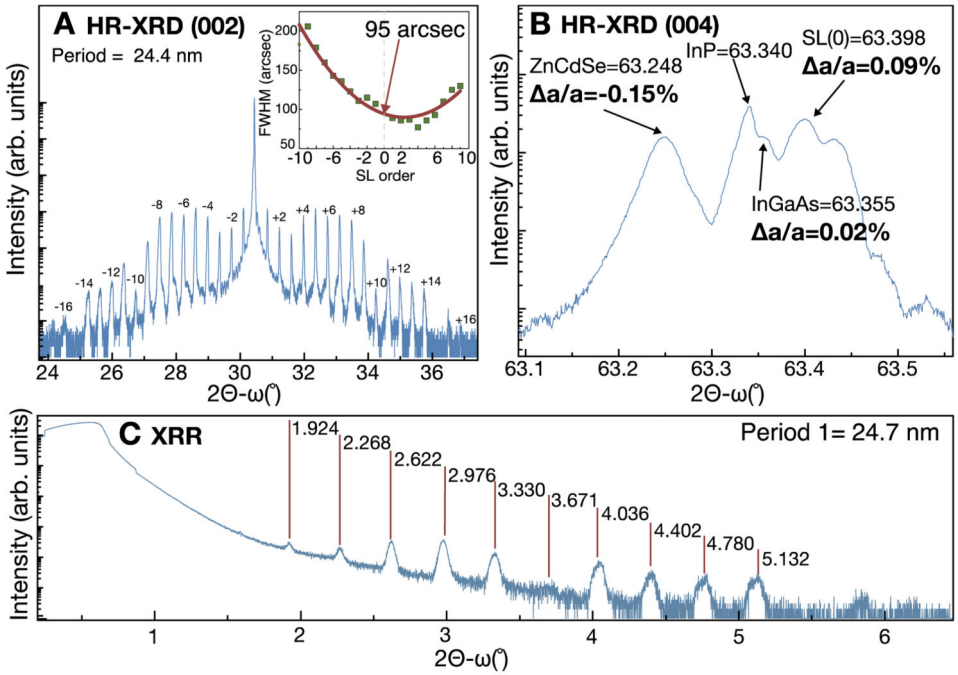

Figure 2.

(A) High resolution x-ray (002) scan of sample showing sharp and strong superlattice fringes and a full width at half maximum polynomial fit of the zero order superlattice peak of 95 arc seconds (inset). (B) High resolution x-scan (004) showing the mismatch of the various layers in the heterostructure. (C) X-ray reflectance(XRR) scan of the structure showing a period of 24.7 nm and good interface quality.

Author Manuscript Author Manuscript Author Manuscript Author Manuscript

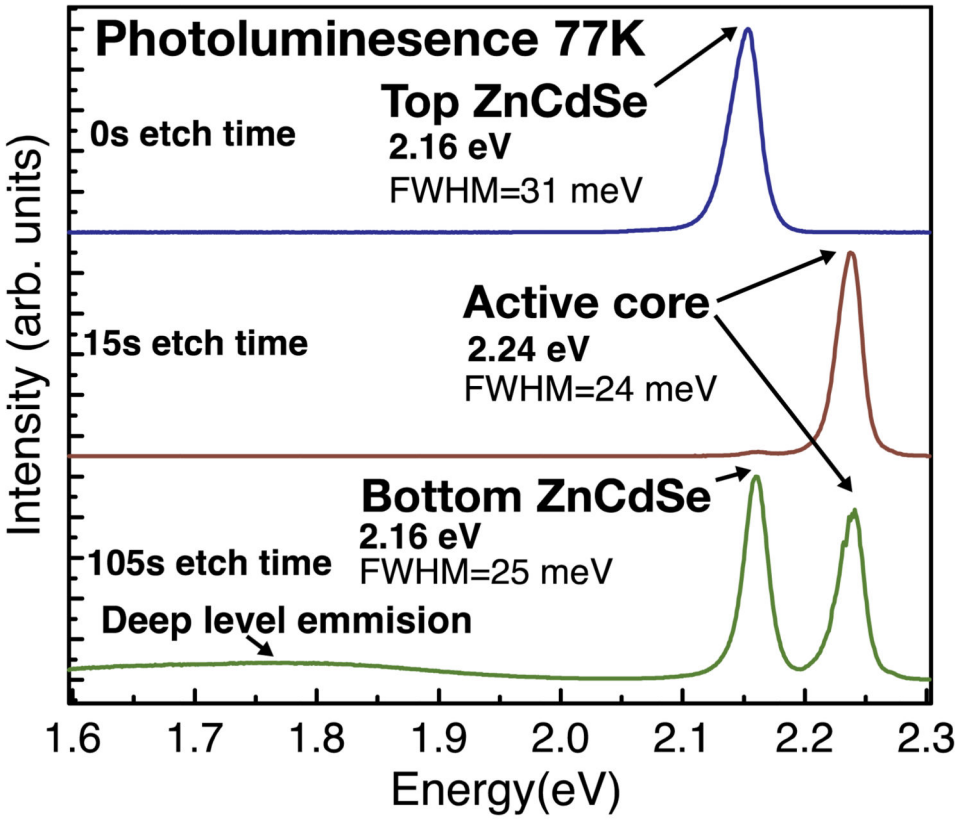

Figure 3.
Photoluminescence spectra at 77K showing bandgap and full width at half maximum changes the sample is etched down the structure.

Author Manuscript Author Manuscript Author Manuscript Author Manuscript

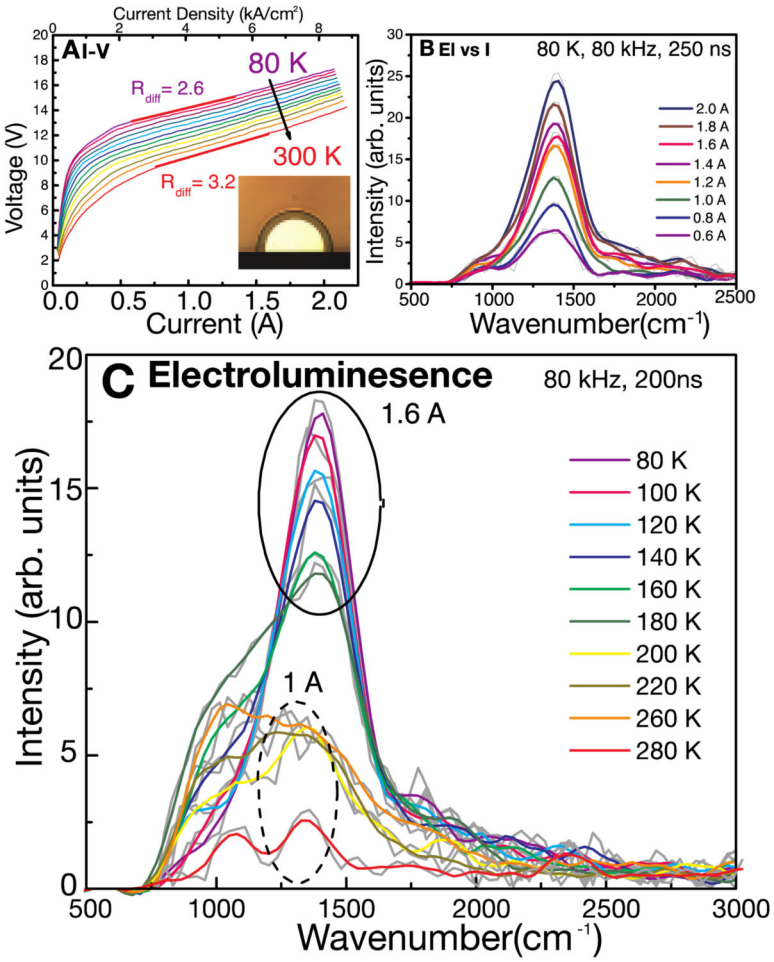

Figure 4.

(A) Pulsed I-V measurements of etched mesa (inset) showing a 11V turn on voltage and 3.2 Ω differential resistance. (B) Current dependence on TM electroluminescence from device at 80K. (C) Temperature dependent electroluminescence spectra showing response up to 280K. Data is indicated in gray, while fitted curves are shown in color.